

SEALS: Sensitivity-driven Efficient Approximate Logic Synthesis

Chang Meng¹, Xuan Wang¹, Jiajun Sun¹, Sijun Tao¹, Wei Wu², Zhihang Wu², Leibin Ni², Xiaolong Shen²,
Junfeng Zhao², and Weikang Qian^{1,3}

¹UM-SJTU Joint Inst. and ³MoE Key Lab of AI, Shanghai Jiao Tong University, China; ²Huawei Technologies Co., China

ABSTRACT

Approximate computing is an emerging computing paradigm to design energy-efficient systems. Many greedy approximate logic synthesis (ALS) methods have been proposed to automatically synthesize approximate circuits. They typically need to consider all local approximate changes (LACs) in each iteration of the ALS flow to select the best one, which is time-consuming. In this paper, we propose SEALS, a Sensitivity-driven Efficient ALS method to speed up a greedy ALS flow. SEALS centers around a newly proposed concept called sensitivity, which enables a fast and accurate error estimation method and an efficient method to filter out unpromising LACs. SEALS can handle any statistical error metric. The experimental results show that it outperforms a state-of-the-art ALS method in runtime by 12× to 15× without reducing circuit quality.

KEYWORDS

approximate computing, approximate logic synthesis, partial difference, sensitivity, error estimation

1 INTRODUCTION

In the post-Moore era, how to sustain the energy-efficiency improvement of computing systems becomes a great challenge. Meanwhile, many error-tolerant applications are widely used today, including image processing, data mining, and machine learning. Under this circumstance, *approximate computing*, an emerging computing paradigm, was proposed to design energy-efficient systems [1, 2]. Its basic idea is to deliberately introduce slight imprecision in computation to improve circuit area, delay, and power consumption.

One topic of approximate computing is *approximate logic synthesis (ALS)*, which aims to find an optimal approximate circuit for a target circuit under a relaxed error bound [3]. Various ALS methods have been proposed [4–13]. Among them, one popular category is the greedy ALS methods due to their good synthesis quality [4, 5, 8, 12]. They iteratively choose the best *local approximate change (LAC)* from the candidate LACs and apply it to the circuit. In [4], by setting a wire as a constant 0 or 1, the circuit is simplified under *error rate (ER)* or *error distance (ED)* constraint. In [5],

an ALS method called SASIMI is proposed, which replaces a signal in the circuit by another almost identical signal or its negation to synthesize an approximate circuit. It can deal with ER or *mean ED (MED)* constraint. In [8], a greedy ALS method is proposed under ER constraint, which is based on Boolean expression simplification of the nodes in a Boolean network. In [12], an ALS approach called ALSRAC is proposed to handle ER or ED constraint. It performs approximate resubstitution to obtain approximate circuits. For all these greedy ALS methods, in each of their iterations, all the candidate LACs in the circuit need to be evaluated, before the best one is selected and applied to the circuit. Thus, if many LACs exist, it takes a long runtime to evaluate all of them.

Notably, all these greedy ALS methods need to evaluate the errors of all the LACs in a circuit in each iteration. It is shown in [14] that an accurate error estimation is important to boost their synthesis quality. Traditionally, the simulation-based method is used for accurate error estimation, which applies each LAC to the current approximate circuit and simulates the new circuit to obtain the errors. However, this method is time-consuming. Thus, more and more attention has been paid to fast error estimation of approximate circuits used within an ALS flow [14–16]. The work [15] propagates the signal distributions of cascaded sub-circuits to estimate the bit error rate of the final output. However, the ED metric is not considered, and the reconvergent paths influence its estimation accuracy. In [16], an error propagation model is applied to each sub-circuit to obtain the maximum ED of the final output. Nevertheless, it cannot handle common statistical error metrics such as ER and MED. In [14], a batch error estimation method based on *Monte Carlo (MC)* simulation and local change propagation is proposed to ensure both the accuracy and efficiency of error estimation. However, as shown in [14], it still takes much time to perform error estimation even for small approximate circuits under ER constraint. Thus, how to improve the speed of a greedy ALS flow while maintaining the error estimation accuracy is still a challenge.

In this paper, to address the aforementioned challenge, we propose SEALS, a Sensitivity-driven Efficient ALS method to speed up the greedy ALS flow. SEALS can be applied to any input distribution, any graph-based circuit representation, and any statistical error metric, such as ER and MED.

The main contributions of our work are as follows.

1. We show that a common operation in a greedy ALS flow, i.e., calculating the error increase by a LAC, can be reduced to calculating a newly proposed metric called sensitivity, which essentially captures how sensitive the error change is with respect to the change of a node value.
2. We further demonstrate that the sensitivities of all the nodes in a circuit can be efficiently obtained, thus enabling an efficient and accurate error estimation. The method to obtain sensitivities is based on calculating another newly proposed metric called partial difference (PD). We show that the PDs of all the nodes in a circuit can be calculated efficiently in a recursive way.

*This work is supported by the National Key R&D Program of China under Grant 2020YFB2205501. Chang Meng (email: changmeng@sjtu.edu.cn) and Xuan Wang (email: xuan.wang@sjtu.edu.cn) contributed equally and should be considered as the co-first authors. Jiajun Sun and Sijun Tao also contributed equally. Corresponding author: Weikang Qian (email: qianwk@sjtu.edu.cn).

Permission to make digital or hard copies of all or part of this work for personal or classroom use is granted without fee provided that copies are not made or distributed for profit or commercial advantage and that copies bear this notice and the full citation on the first page. Copyrights for components of this work owned by others than ACM must be honored. Abstracting with credit is permitted. To copy otherwise, or republish, to post on servers or to redistribute to lists, requires prior specific permission and/or a fee. Request permissions from permissions@acm.org.
DAC '22, July 10–14, 2022, San Francisco, CA, USA

© 2022 Association for Computing Machinery.
ACM ISBN 978-1-4503-9142-9/22/07...\$15.00
<https://doi.org/10.1145/3489517.3530464>

3. We propose the entire SEALS flow, which applies sensitivities to calculate the error increases of LACs. It also applies an efficient LAC filtering method for acceleration. The method filters out the nodes with high sensitivities and the LACs with large error increases, thus greatly reducing the number of candidate LACs that need to be accurately evaluated in each iteration.

The experimental results show that compared with a state-of-the-art method, SEALS accelerates by 12× to 15× under three different error metrics over a wide range of circuits.

The rest of the paper is organized as follows. Section 2 elaborates our method to calculate error increase, which is a key component in SEALS. Section 3 presents the SEALS methodology. Section 4 shows the experimental results. Section 5 concludes the paper.

2 CALCULATING ERROR INCREASE

This section presents a key step in SEALS, which is to calculate the error increase of a given circuit due to an applied LAC.

2.1 Error Increase Calculation and Sensitivity

This section shows that the error increase calculation can be reduced to calculating a newly defined metric called sensitivity. We first describe some assumptions and notations used in this paper.

- In order to flexibly handle any input distribution and any large circuit, the error estimation is based on MC simulation [14]. Assume that m random input patterns are sampled from the given input distribution. We refer to the i -th ($1 \leq i \leq m$) random input pattern as *input pattern i* .
- Denote the original input circuit as \mathcal{G}_{org} and the current approximate circuit (i.e., the given circuit) as \mathcal{G} .
- Denote the set of nodes in \mathcal{G} as N and the set of POs of \mathcal{G} as O .
- Suppose that a LAC ψ is applied to \mathcal{G} and the resulting new approximate circuit is \mathcal{G}_{new} .
- Suppose that the LAC ψ affects a local circuit \mathcal{K} in the current circuit \mathcal{G} ($\mathcal{K} \subseteq \mathcal{G}$) and the resulting new local circuit is \mathcal{K}_{new} ($\mathcal{K}_{new} \subseteq \mathcal{G}_{new}$). One assumption in our work is that we only consider LACs such that the affected local circuits have a single output. We note that many existing LACs satisfy this property, such as those proposed in [4, 5, 8, 12].
- Denote the single output node of \mathcal{K} and \mathcal{K}_{new} as n and n_{new} , respectively. Denote their values under input pattern i as $V_n(i)$ and $V_{n_{new}}(i)$, respectively.
- Denote the binary numbers represented by the POs of \mathcal{G}_{org} , \mathcal{G} , and \mathcal{G}_{new} under input pattern i as $Y_{org}(i)$, $Y(i)$, and $Y_{new}(i)$, respectively.
- In our proposed method, we simulate circuits with the m random input patterns to obtain some values to be used later. Specifically, we simulate the original circuit \mathcal{G}_{org} to obtain an *output value vector* $\vec{Y}_{org} = (Y_{org}(1), \dots, Y_{org}(m))$. We also simulate the current approximate circuit \mathcal{G} to obtain a node value matrix \mathbf{M} . Each entry in \mathbf{M} , denoted as $M[i, n]$ ($1 \leq i \leq m, n \in N$), represents the value of node n under input pattern i .
- Denote the error between two values v_1 and v_2 as $f(v_1, v_2)$.

With the MC simulation, the error of \mathcal{G} can be calculated as $\frac{1}{m} \sum_{i=1}^m f(Y(i), Y_{org}(i))$ and that of \mathcal{G}_{new} can be calculated similarly. Note that with a proper choice of f , various error metrics can be calculated. For example, if $f(v_1, v_2)$ returns 1 if $v_1 \neq v_2$ and 0 otherwise, then ER is calculated.

For the LAC ψ , we want to calculate the *error increase* $\Delta E(\psi)$ between \mathcal{G}_{new} and \mathcal{G} , which equals the error of \mathcal{G}_{new} minus that of \mathcal{G} . With the MC simulation, it can be calculated as follows:

$$\Delta E(\psi) = \frac{1}{m} \sum_{i=1}^m (f(Y_{new}(i), Y_{org}(i)) - f(Y(i), Y_{org}(i))). \quad (1)$$

To calculate ΔE by Eq. (1), it reduces to calculating the expression $e_1 = f(Y_{new}(i), Y_{org}(i)) - f(Y(i), Y_{org}(i))$, which is essentially the error increase under input pattern i . Next, we prove that $e_1 = e_2$, with e_2 as follows:

$$e_2 = (V_{n_{new}}(i) - V_n(i)) \times (f(\hat{Y}(i, V_n = 1), Y_{org}(i)) - f(\hat{Y}(i, V_n = 0), Y_{org}(i))), \quad (2)$$

where $\hat{Y}(i, V_n = u)$ ($u \in \{0, 1\}$) is the binary number represented by the POs of \mathcal{G} under input pattern i , if we set the value of n as u .

It can be proved by considering the following 3 cases:

1. The case where $V_n(i) = V_{n_{new}}(i)$. In this case, the LAC ψ does not change the output value of the local circuit under input pattern i , and hence, does not affect the POs. Thus, the error increase e_1 is 0. Since $V_n(i) = V_{n_{new}}(i)$, by Eq. (2), we also have $e_2 = 0 = e_1$.
2. The case where $V_n(i) = 0$ and $V_{n_{new}}(i) = 1$. In this case, the LAC ψ causes a 0 to 1 change on the output n of the local circuit under input pattern i . The binary number represented by the POs of the current approximate circuit changes from $\hat{Y}(i, V_n = 0)$ to $\hat{Y}(i, V_n = 1)$, and hence, the error increase e_1 should be $(f(\hat{Y}(i, V_n = 1), Y_{org}(i)) - f(\hat{Y}(i, V_n = 0), Y_{org}(i)))$, which equals e_2 .
3. The case where $V_n(i) = 1$ and $V_{n_{new}}(i) = 0$. It is symmetric to case 2 and the claim can be proved similarly.

An important component in Eq. (2) is

$$\Delta L[i, n] = f(\hat{Y}(i, V_n = 1), Y_{org}(i)) - f(\hat{Y}(i, V_n = 0), Y_{org}(i)). \quad (3)$$

It represents the error increase by changing the value of n from 0 to 1. Intuitively, if $\Delta L[i, n]$ is larger, then the value change on node n will cause a larger change on error, and hence, the error is more sensitive to the node n . Thus, we refer to $\Delta L[i, n]$ as *error sensitivity*, or sensitivity in short. The values of $\Delta L[i, n]$ for all the m random input patterns and all the nodes in \mathcal{G} form a *sensitivity matrix (SM)* $\Delta \mathbf{L}$. We will show how to obtain the SM in Section 2.2.

Based on the above discussion, the error increase $\Delta E(\psi)$ by a LAC can be obtained through the SM by the function *ErrorEstimate* shown in Algorithm 1. The inputs of Algorithm 1 are a LAC ψ , the current approximate circuit \mathcal{G} , the node value matrix \mathbf{M} of \mathcal{G} obtained from the MC simulation, and the SM $\Delta \mathbf{L}$. The output is the estimated error increase $\Delta E(\psi)$ by the LAC ψ .

Algorithm 1: The function *ErrorEstimate*($\psi, \mathcal{G}, \mathbf{M}, \Delta \mathbf{L}$) to estimate the error increase by a LAC.

Input: a LAC ψ , a circuit \mathcal{G} , a node value matrix \mathbf{M} of size $m \times |N|$, and an SM $\Delta \mathbf{L}$.

Output: estimated error increase $\Delta E(\psi)$.

- 1 (n, n_{new}) \leftarrow outputs of local circuits \mathcal{K} and \mathcal{K}_{new} affected by ψ ;
 - 2 Obtain the signal value vector \vec{V}_n of n from \mathbf{M} ;
 - 3 Obtain the signal value vector $\vec{V}_{n_{new}}$ of n_{new} by simulating \mathcal{K}_{new} ;
 - 4 $\Delta E(\psi) \leftarrow 0$;
 - 5 **for** i from 1 to m **do**
 - 6 | $\Delta E(\psi) \leftarrow \Delta E(\psi) + (V_{n_{new}}(i) - V_n(i)) \cdot \Delta L[i, n]$;
 - 7 **return** $\Delta E(\psi)$;
-

In Algorithm 1, Line 1 identifies the output nodes n and n_{new} of the local circuits \mathcal{K} and \mathcal{K}_{new} affected by the LAC ψ , respectively. We use two *signal value vectors* \vec{V}_n and $\vec{V}_{n_{new}}$ to store the values of the nodes n and n_{new} under all the m random input patterns, respectively. Line 2 obtains \vec{V}_n from the node value matrix \mathbf{M} . Line 3 obtains $\vec{V}_{n_{new}}$ by simulating the local circuit \mathcal{K}_{new} with inputs taken from \mathbf{M} . Since \mathcal{K}_{new} is usually small, the simulation process only costs little time. Then, Lines 4–6 accumulate the error increase by the LAC ψ based on Eqs. (2) and (3).

2.2 Obtaining Sensitivity

We show how to obtain the SM ΔL in this section. By Eq. (3), we need to obtain $\hat{Y}(i, V_n = 1)$, $\hat{Y}(i, V_n = 0)$, and $Y_{org}(i)$ to calculate $\Delta L[i, n]$. As we stated in Section 2.1, $Y_{org}(i)$ is obtained by the MC simulation. Thus, we focus on obtaining $\hat{Y}(i, V_n = 1)$ and $\hat{Y}(i, V_n = 0)$. Next, we show how to obtain them by first considering the case where $V_n(i) = 1$. Since $V_n(i) = 1$, by definition, we have

$$\hat{Y}(i, V_n = 1) = Y(i). \quad (4)$$

With the node value matrix \mathbf{M} available, we can get the values of all the POs of \mathcal{G} and then get the value of $Y(i)$. To obtain $\hat{Y}(i, V_n = 0)$, a direct method is to simulate \mathcal{G} again by flipping the value of n under input pattern i , which is time-consuming. Instead, we propose to obtain $(\hat{Y}(i, V_n = 1) - \hat{Y}(i, V_n = 0))$ first, which is called *PD*. We use a two-dimensional *PD matrix (PDM)* ΔY to store the PD for each node $n \in N$ under each random input pattern. Each entry in ΔY is denoted as:

$$\Delta Y[i, n] = \hat{Y}(i, V_n = 1) - \hat{Y}(i, V_n = 0). \quad (5)$$

Different from Boolean difference, which indicates whether a change of an internal node causes a change on POs or not, PD gives the exact magnitude change of the binary number represented by the POs with respect to an internal node change. We will show an efficient method to get the PDM in Section 2.3. Now, we assume that the PDM is obtained. Then, by Eqs. (4) and (5), we can get

$$\hat{Y}(i, V_n = 0) = \hat{Y}(i, V_n = 1) - \Delta Y[i, n] = Y(i) - \Delta Y[i, n]. \quad (6)$$

Then, by Eqs. (3), (4), and (6), we can get the sensitivity

$$\Delta L[i, n] = f(Y(i), Y_{org}(i)) - f(Y(i) - \Delta Y[i, n], Y_{org}(i)). \quad (7)$$

For the other case where $V_n(i) = 0$, we can similarly get

$$\Delta L[i, n] = f(Y(i) + \Delta Y[i, n], Y_{org}(i)) - f(Y(i), Y_{org}(i)). \quad (8)$$

Based on the above discussion, we present the procedure *GetSenMatrix* to get the SM ΔL in Algorithm 2. The inputs are the current approximate circuit \mathcal{G} , the node value matrix \mathbf{M} of \mathcal{G} , and the output value vector \vec{Y}_{org} of the original circuit \mathcal{G}_{org} . The output is the SM ΔL . In Algorithm 2, Line 1 applies the method to be described in Section 2.3 to calculate the PDM ΔY of \mathcal{G} based on the matrix \mathbf{M} . Then, for each $1 \leq i \leq m$, Line 3 extracts the value $Y_{org}(i)$ from \vec{Y}_{org} , and calculates the approximate output value $Y(i)$ from \mathbf{M} . Then, for each node n in \mathcal{G} , if $M[i, n] = 1$, which means that $V_n(i) = 1$, Line 5 calculates $\Delta L[i, n]$ by Eq. (7). Otherwise, Line 6 computes $\Delta L[i, n]$ by Eq. (8).

2.3 Obtaining Partial Difference Matrix

This section presents our proposed efficient method to obtain the PDM. It obtains the PD for each node $n \in N$ in a reverse topological order of the circuit. First, the PD for each PO is obtained. Denote the k -th ($0 \leq k < |O|$) node in the PO set O of \mathcal{G} as o_k ,

Algorithm 2: The function *GetSenMatrix*(\mathcal{G} , \mathbf{M} , \vec{Y}_{org}) to calculate the SM ΔL .

Input: a circuit \mathcal{G} , a node value matrix \mathbf{M} of size $m \times |N|$, and an output value vector \vec{Y}_{org} .
Output: the SM ΔL .

```

1  $\Delta Y \leftarrow$  GetPartialDiffMatrix( $\mathcal{G}$ ,  $\mathbf{M}$ );
2 for  $i$  from 1 to  $m$  do
3   obtain  $Y_{org}(i)$  from  $\vec{Y}_{org}$ ; calculate  $Y(i)$  from  $\mathbf{M}$ ;
4   foreach node  $n$  in  $\mathcal{G}$  do
5     if  $M[i, n] = 1$  then
6        $\Delta L[i, n] \leftarrow f(Y(i), Y_{org}(i)) - f(Y(i) - \Delta Y[i, n], Y_{org}(i));$ 
7     else
8        $\Delta L[i, n] \leftarrow f(Y(i) + \Delta Y[i, n], Y_{org}(i)) - f(Y(i), Y_{org}(i));$ 
9   return  $\Delta L$ ;
```

which has a weight of 2^k in the binary representation. By Eq. (5) and the definition of $\hat{Y}(i, V_n = u)$, we have

$$\Delta Y[i, o_k] = \hat{Y}(i, V_{o_k} = 1) - \hat{Y}(i, V_{o_k} = 0) = 2^k. \quad (9)$$

Next, we present our method for calculating the PD for each node $n \in N \setminus O$. We begin with some definitions.

- In a circuit, if there exists a path from node A to B , then B is a *transitive fanout (TFO)* of A .
- A *cut* of a node n in a circuit is a set of nodes in the circuit satisfying that 1) each path from n to a PO passes at least one node in the set and 2) no node in the set can be removed without violating condition 1.
- The *disjoint cut* S_n for a node n is a cut not equal to $\{n\}$ but closest to n satisfying that the TFOs of all nodes in the cut have no mutual intersection.

To obtain the disjoint cut for a node n , a node set S_n is initialized as the direct fanouts of n . If the TFOs of some nodes in S_n intersect, then the node $c \in S_n$ with the smallest topological order is removed from S_n , and c 's fanouts are added into S_n . We repeat this step until the TFOs of all nodes in S_n have no mutual intersection.

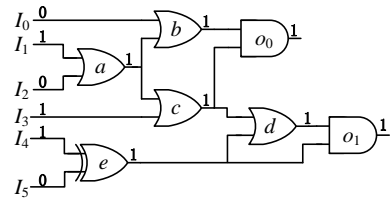


Figure 1: An example circuit.

EXAMPLE 1. Consider an example circuit in Fig. 1. A topological order of it is $I_0, I_1, I_2, I_3, I_4, I_5, a, e, b, c, d, o_0, o_1$. We want to get the disjoint cut S_a for node a . S_a is initialized as the direct fanouts of node a , i.e., $S_a = \{b, c\}$. However, the TFOs of b and c intersect at node o_0 . Since b precedes c in the topological order, we replace b by its direct fanout o_0 , and S_a is updated to $S_a = \{c, o_0\}$. This step is repeated until the TFOs of all nodes in S_a have no intersection. Finally, we obtain the disjoint cut for node a is $S_a = \{d, o_0\}$. For node d , we can obtain its disjoint cut as $S_d = \{o_1\}$ in a similar way.

For any two nodes n and c in the node set N of \mathcal{G} , we also define a *local PD* of c with respect to n as

$$\Delta W_c[i, n] = W_c(i, V_n = 1) - W_c(i, V_n = 0), \quad (10)$$

where $W_c(i, V_n = u)$ ($u \in \{0, 1\}$) is the value of node c under input pattern i if we set the value of n as u .

Our method to calculate the PD of a node $n \in N \setminus O$ is based on the theorem below.

THEOREM 1. For a node $n \in N \setminus O$, we have

$$\Delta Y[i, n] = \sum_{c \in S_n} \Delta Y[i, c] \Delta W_c[i, n], \quad (11)$$

where S_n is the disjoint cut of n .

PROOF. In the proof, we focus on one specific input pattern, so the input pattern index i is omitted for simplicity.

Suppose that $S_n = \{c_1, \dots, c_r\}$ and for $1 \leq j \leq r$, the set of POs that are TFOs of c_j is O_j . By the definition of disjoint cut, the sets O_1, \dots, O_r are mutually disjoint. Let $\Omega = \bigcup_{j=1}^r O_j$. Clearly, Ω is the set of POs that are TFOs of n .

By the definition of $\hat{Y}(V_n = u)$ and $W_c(V_n = u)$, we have

$$\hat{Y}(V_n = u) = \sum_{o_k \in O} 2^k W_{o_k}(V_n = u), \quad \forall u \in \{0, 1\}. \quad (12)$$

For any $o_k \in O \setminus \Omega$, since o_k is not a TFO of n , we have $W_{o_k}(V_n = 1) = W_{o_k}(V_n = 0)$. Combining this fact with Eqs. (5), (10), and (12), we have

$$\begin{aligned} \Delta Y[n] &= \hat{Y}(V_n = 1) - \hat{Y}(V_n = 0) \\ &= \sum_{o_k \in \Omega} 2^k (W_{o_k}(V_n = 1) - W_{o_k}(V_n = 0)) = \sum_{o_k \in \Omega} 2^k \Delta W_{o_k}[n]. \end{aligned} \quad (13)$$

Similarly, we can get that for any $c_j \in S_n$,

$$\Delta Y[c_j] = \sum_{o_k \in O_j} 2^k \Delta W_{o_k}[c_j]. \quad (14)$$

Now, we prove that for any $o_k \in O_j$,

$$\Delta W_{o_k}[c_j] \Delta W_{c_j}[n] = \Delta W_{o_k}[n]. \quad (15)$$

We distinguish among 3 possible cases of $\Delta W_{c_j}[n]$.

1. $\Delta W_{c_j}[n] = 0$. By Eq. (10), we have $W_{c_j}(V_n = 1) = W_{c_j}(V_n = 0)$, which means that c_j is a constant independent of the value of n . Since c_j is a node in the disjoint cut S_n , all paths from n to o_k pass through c_j . Thus, o_k is also a constant independent of the value of n , i.e., $W_{o_k}(V_n = 1) = W_{o_k}(V_n = 0)$. Thus, by Eq. (10), $\Delta W_{o_k}[n] = 0 = \Delta W_{o_k}[c_j] \Delta W_{c_j}[n]$.
2. $\Delta W_{c_j}[n] = 1$. By Eq. (10), we must have $W_{c_j}(V_n = 1) = 1$ and $W_{c_j}(V_n = 0) = 0$. Thus, the value of node c_j equals that of node n . Since as mentioned above, all paths from n to o_k pass through c_j , we have that for any $u \in \{0, 1\}$, $W_{o_k}(V_n = u) = W_{o_k}(V_{c_j} = u)$. By Eq. (10), we have $\Delta W_{o_k}[n] = \Delta W_{o_k}[c_j] = \Delta W_{o_k}[c_j] \Delta W_{c_j}[n]$.
3. $\Delta W_{c_j}[n] = -1$. This case is symmetric to case 2 and the claim can be proved similarly.

By Eqs. (13), (14), and (15), we finally conclude that

$$\begin{aligned} \Delta Y[n] &= \sum_{o_k \in \Omega} 2^k \Delta W_{o_k}[n] = \sum_{c_j \in S_n} \sum_{o_k \in O_j} 2^k \Delta W_{o_k}[n] \\ &= \sum_{c_j \in S_n} \sum_{o_k \in O_j} 2^k \Delta W_{o_k}[c_j] \Delta W_{c_j}[n] = \sum_{c_j \in S_n} \Delta Y[c_j] \Delta W_{c_j}[n]. \end{aligned}$$

By Theorem 1, we can simply calculate the PDs of all nodes $n \in N \setminus O$ in a reverse topological order of the circuit based on Eq. (11), starting from $\Delta Y[i, o_k]$'s for $o_k \in O$, which are obtained by Eq. (9). In order to apply Eq. (11), we also need to obtain the local PD for each node c in the disjoint cut S_n with respect to n . By Eq. (10), we need to get $W_c(i, V_n = 1)$ and $W_c(i, V_n = 0)$. We first extract one of

them from the node value matrix \mathbf{M} based on the actual value of n , and then get the other by flipping the value of the node n and simulating the local circuit between n and c . Note that the local circuit is usually small, so the simulation process takes little time.

Below shows an example of getting PDs by Eq. (11).

EXAMPLE 2. Consider an example circuit in Fig. 1. Assume that input pattern i is $I_0 I_1 \dots I_5 = 010110$. The value of each wire is shown above the wire under this input pattern. We want to calculate PD $\Delta Y[i, a]$ for node a . From Example 1, the disjoint cut of node a is $S_a = \{d, o_0\}$ and that of d is $S_d = \{o_1\}$. By Eq. (9), $\Delta Y[i, o_1] = 2^1 = 2$ and $\Delta Y[i, o_0] = 2^0 = 1$. By Eq. (10), $\Delta W_{o_1}[i, d] = W_{o_1}(i, V_d = 1) - W_{o_1}(i, V_d = 0) = 1$, $\Delta W_d[i, a] = 0$, and $\Delta W_{o_0}[i, a] = 1$. Thus, by Eq. (11), we have $\Delta Y[i, d] = \Delta Y[i, o_1] \Delta W_{o_1}[i, d] = 2$ and

$$\Delta Y[i, a] = \Delta Y[i, d] \Delta W_d[i, a] + \Delta Y[i, o_0] \Delta W_{o_0}[i, a] = 1.$$

3 SEALS METHODOLOGY

This section presents the proposed SEALS method to speed up the iterative greedy ALS flow. The procedure of SEALS is shown in Algorithm 3. The inputs are an original circuit \mathcal{G}_{org} , an error bound e_b , a node number ratio l_n , and a LAC number ratio l_r . The output is an approximate circuit \mathcal{G} with error no more than e_b . The algorithm uses two kinds of MC simulations: 1) MC simulation with a small number of input patterns for quickly filtering out some unpromising LACs (Lines 4–12); 2) MC simulation with a large number of input patterns for accurate error estimation (Lines 13–18).

Algorithm 3: The proposed flow of SEALS.

Input: an original circuit \mathcal{G}_{org} , an error bound e_b , a node number ratio l_n , and a LAC number ratio l_r .
Output: an approximate circuit \mathcal{G} with error $e \leq e_b$.

- 1 $\mathcal{G}_{new} \leftarrow \mathcal{G}_{org}$; $e \leftarrow 0$;
- 2 **while** $e \leq e_b$ **do**
- 3 $\mathcal{G} \leftarrow \mathcal{G}_{new}$;
- 4 generate a small set Z_1 of J random input patterns;
- 5 simulate \mathcal{G}_{org} with Z_1 to obtain the output value vector \vec{Y}_{org1} ;
- 6 simulate \mathcal{G} with Z_1 to obtain the node value matrix \mathbf{M}_1 ;
- 7 $\Delta L_1 \leftarrow \text{GetSetMatrix}(\mathcal{G}, \mathbf{M}_1, \vec{Y}_{org1})$;
- 8 qualified node set $S_n \leftarrow \text{NodeFilter}(\mathcal{G}, \Delta L_1, l_n)$;
- 9 identify candidate LAC set S_D from S_n ;
- 10 **foreach** candidate LAC ψ in S_D **do**
- 11 $\Delta E_1[\psi] \leftarrow \text{ErrorEstimate}(\psi, \mathcal{G}, \mathbf{M}_1, \Delta L_1)$;
- 12 qualified LAC set $S_\psi \leftarrow \text{LACFilter}(S_D, \Delta E_1, l_r)$;
- 13 generate a large set Z_2 of K random input patterns;
- 14 simulate \mathcal{G}_{org} with Z_2 to obtain the output value vector \vec{Y}_{org2} ;
- 15 simulate \mathcal{G} with Z_2 to obtain the node value matrix \mathbf{M}_2 ;
- 16 $\Delta L_2 \leftarrow \text{GetSetMatrix}(\mathcal{G}, \mathbf{M}_2, \vec{Y}_{org2})$;
- 17 **foreach** qualified LAC ψ in S_ψ **do**
- 18 $\Delta E_2[\psi] \leftarrow \text{ErrorEstimate}(\psi, \mathcal{G}, \mathbf{M}_2, \Delta L_2)$;
- 19 choose the LAC ψ^* with the smallest $\Delta E_2[\psi^*]$ and then apply it to a copy of \mathcal{G} to obtain \mathcal{G}_{new} ;
- 20 calculate the accurate error e between \mathcal{G}_{new} and \mathcal{G}_{org} ;
- 21 **return** \mathcal{G} ;

In Algorithm 3, Line 1 initializes the new circuit \mathcal{G}_{new} as the original circuit \mathcal{G}_{org} , and sets the actual error e of \mathcal{G}_{new} as 0. In the main loop, Line 3 sets the current approximate circuit \mathcal{G} as \mathcal{G}_{new} . Line 4 generates a small number of J random input patterns by sampling a given input distribution. Lines 5–6 apply them to

simulate the circuits \mathcal{G}_{org} and \mathcal{G} to obtain the output value vector \vec{Y}_{org1} and the node value matrix \mathbf{M}_1 , respectively.

Based on the MC simulation with a small number of J input patterns, Lines 7–8 first filter out some unpromising nodes with high sensitivities to obtain the qualified node set S_n . Then, for each node in S_n , Lines 9–12 filter out some unpromising LACs with large error increases to obtain the qualified LAC set S_ψ . Specifically, Line 7 first calls the function *GetSenMatrix* shown in Algorithm 2 to obtain the SM ΔL_1 for the current approximate circuit \mathcal{G} based on \mathbf{M}_1 and \vec{Y}_{org1} . According to the SM ΔL_1 and the node number ratio l_n , Line 8 calls the function *NodeFilter* to filter some unpromising nodes to obtain the qualified node set S_n for \mathcal{G} . At this moment, without knowing the actual LACs, this function just calculates an *upper bound* on the error increase by any LAC ψ_n applied to a node n . Specifically, by Eqs. (1), (2), and (3), we have the error increase of ψ_n , $\Delta E(\psi_n) \leq \frac{1}{J} \sum_{i=1}^J |\Delta L_1[i, n]|$. We call the upper bound on $\Delta E(\psi_n)$ the *node sensitivity* of n . Thus, this function first calculates the node sensitivity of each node n in \mathcal{G} as $\frac{1}{J} \sum_{i=1}^J |\Delta L_1[i, n]|$. Then, it picks $l_n|N|$ nodes with the lowest node sensitivities to form the qualified node set S_n . Then, Line 9 identifies the candidate LAC set S_D only on the nodes in the set S_n . Note that the actual type of LAC can be any existing one such as those proposed in [4, 5, 8, 12], as long as its affected local circuits have a single output. Then, for each candidate LAC ψ in S_D , Line 11 calls the function *ErrorEstimate* shown in Algorithm 1 to estimate the error increase $\Delta E_1[\psi]$ based on \mathbf{M}_1 and the SM ΔL_1 . Then, Line 12 calls the function *LAC-Filter* to obtain the qualified LAC set S_ψ based on the candidate LAC set S_D , the estimated error increase ΔE_1 , and the LAC number ratio l_r . This function picks $l_r|S_D|$ LACs in S_D with the smallest error increases to construct the qualified node set S_ψ .

After obtaining the qualified LAC set S_ψ , Lines 13–18 perform a round of more accurate estimate of the error increases of the LACs in S_ψ . It is similar to Lines 4–7 and 10–11 and still based on the SM. The main difference is that a large number of K random input patterns are used (see Line 13). Then, Line 19 chooses the LAC ψ^* with the smallest error increase and then applies it to a copy of \mathcal{G} to obtain the new approximate circuit \mathcal{G}_{new} . Finally, Line 20 calculates the actual error e between \mathcal{G}_{new} and \mathcal{G}_{org} . When the error e is no more than the error bound e_b , the loop will continue (see Line 2). Otherwise, Line 21 returns the latest approximate circuit \mathcal{G} .

4 EXPERIMENTAL RESULTS

This section shows the experimental results of SEALS. All the experiments are conducted on a 16-core AMD 5950X processor running at 2.2GHz with 64GB RAM. The small number J , the large number K , the node number ratio l_n , and the LAC number ratio l_r in Algorithm 3 are set as 2^{10} , 2^{17} , 0.5, and 0.1, respectively. The primary inputs are assumed to be uniformly distributed, although SEALS can deal with any input distribution. We consider three representative statistical error metrics, i.e., ER, *normalized MED* (NMED) and *mean relative ED* (MRED) [12].

The benchmarks used in our experiments include some IS-CAS [17] and arithmetic circuits, which are listed in Table 1 along with their areas and delays. The area and delay of each circuit are normalized to the area and delay of the INV_X1 gate in the MCNC library [18], respectively. The *area ratio* (i.e., the area of the approximate circuit over that of the accurate one) and the *delay ratio* (i.e.,

Table 1: Benchmarks used in our experiments.

Circuit	Area	Delay	Circuit	Area	Delay	Circuit	Area	Delay
alu4	2798	12.7	c880	585	24.9	mtp8	1069	37.8
c1908	758	37.3	cla32	958	38.5	rca32	666	16.1
c3540	1604	55.0	ksa32	1128	17.8	wal8	1081	45.3

the delay of the approximate circuit over that of the accurate one) are used to evaluate the quality of approximate circuits. In addition, the runtimes of the algorithms are reported. To take randomness into account, each experiment is repeated three times and the average results are reported.

We compare SEALS with a state-of-the-art method, called Su’s method [14], which applies batch error estimation method to improve the error estimation accuracy and speed up the greedy ALS flow. Su’s method is also based on MC simulation and we set its number of random input patterns as 10^5 , which is a little smaller than the value K in SEALS. The type of LAC used in both SEALS (see Line 9 of Algorithm 3) and Su’s method is the one from [5], which replaces a signal in a circuit with another signal or its negation. To select the best LAC in each iteration, Su’s method uses the same criterion as [5]. Since Su’s method is relatively slow, for a fair comparison, we also add a LAC filter to it. Su’s method does not calculate sensitivity values, so the same filters as SEALS are not added to it. Instead, we add a filter that filters out each LAC such that the pair of signals involved in the LAC do not share a common dependent primary input. Note that the pair of signals involved in such a LAC are very likely to be quite different, and hence, the LAC is not a promising choice.

4.1 Performance under ER Constraint

In this section, we compare SEALS with Su’s method under ER constraint for all the circuits in Table 1. Note that Su’s method uses a three-dimensional 0-1 matrix to indicate whether an internal approximation error will influence the value of each PO in the circuit. Thus, under ER constraint, bit-parallel operation can be applied to accelerate it, which realizes concurrent computation for different rounds of logic simulation. Therefore, we implement two versions of Su’s method: 1) *without bit-parallel operation* (w/o BP), which is the same as the implementation in [14]; 2) *with bit-parallel operation* (w/ BP), which is the enhanced version of Su’s method.

Table 2 lists the average area and delay ratios and the average runtime of SEALS and Su’s method under ER constraint. For Su’s methods w/o BP and w/ BP, the area and delay of an approximate circuit synthesized by them are identical. Thus, Table 2 lists only one column for the average area/delay ratio of Su’s method (named Su’s). The values for each circuit are the average results under 7 ER thresholds (0.1%, 0.3%, 0.5%, 0.8%, 1%, 3%, 5%). We highlight the data in **bold** when SEALS performs better than Su’s method. Similar notations are applied in the following tables. From Table 2, for nearly half of the benchmarks, SEALS synthesizes approximate circuits with smaller area and shorter delay than Su’s method. All the circuits except alu4 synthesized by SEALS have either smaller areas or shorter delays, where at least one quantity is largely improved and the other is slightly worse. In terms of runtime, SEALS is **14**× faster than Su’s method w/o BP on average. Since SEALS uses SM that stores binary radix numbers, the bit parallel operation cannot

be applied to it under ER constraint. However, no significant runtime difference exists between SEALS and Su’s method w/ BP.

Table 2: Comparison of SEALS and Su’s methods w/o BP and w/ BP under ER constraint.

circuit	Aver. area ratio		Aver. delay ratio		Average time (s)		
	Su’s	SEALS	Su’s	SEALS	Su’s w/o BP	Su’s w/ BP	SEALS
alu4	76.92%	80.09%	100.00%	102.14%	9012	828	424
c1908	81.47%	79.40%	90.46%	79.62%	290	23	68
c3540	94.26%	94.04%	100.00%	89.64%	1379	119	161
c880	94.82%	96.41%	97.93%	85.66%	50	4	17
cla32	86.65%	72.38%	78.18%	78.52%	316	27	84
ksa32	88.16%	85.49%	95.75%	88.04%	658	56	67
mtp8	96.11%	97.82%	98.94%	95.88%	360	33	27
rca32	98.03%	96.44%	99.38%	99.47%	17	2	4
wal8	96.15%	89.35%	93.82%	84.30%	599	57	39
Avg	90.29%	87.94%	94.94%	89.25%	1409	128	99

4.2 Performance under NMED Constraint

This section compares SEALS with Su’s method under NMED constraint. Since NMED is an error metric for arithmetic circuits, only such circuits in Table 1 are selected. Note that when calculating the error metrics related to ED, such as NMED and MRED, we need to use the binary number represented by the POs to calculate the final error magnitude. Thus, bit parallel operation is not applicable for these error metrics for both SEALS and Su’s method.

Table 3 lists the average area and delay ratios and the average runtime of SEALS and Su’s method under NMED constraint. The values for each benchmark are the average results under 8 NMED thresholds (0.00153%, 0.00305%, 0.00610%, 0.01221%, 0.02441%, 0.04883%, 0.09766%, 0.19531%). From Table 3, all the approximate circuits obtained by SEALS except mtp8 have smaller areas than those obtained by Su’s method. In an average sense, SEALS synthesizes approximate circuits with both smaller area and delay than Su’s method. Furthermore, SEALS dramatically reduces the runtime over Su’ method for all the circuits. On average, SEALS is 12× faster than Su’s method.

Table 3: Comparison of SEALS and Su’s method under NMED constraint.

circuit	Average area ratio		Average delay ratio		Average time (s)	
	Su	SEALS	Su	SEALS	Su	SEALS
cla32	25.22%	22.05%	51.07%	61.17%	2861	259
ksa32	27.35%	24.59%	79.85%	81.60%	6090	302
mtp8	82.45%	83.55%	97.62%	89.35%	1122	178
rca32	29.11%	28.47%	98.52%	92.70%	1165	148
wal8	77.69%	66.57%	89.18%	86.62%	2003	174
Avg	48.36%	45.05%	83.25%	82.29%	2648	212

4.3 Performance under MRED Constraint

This section compares SEALS with Su’s method under MRED constraint. Same as NMED, since MRED is an error metric for arithmetic circuits, we only choose such circuits in Table 1. Table 4

lists the average area and delay ratios and the average runtime of SEALS and Su’s method under MRED constraint. The values for each benchmark are the average results under 8 MRED thresholds same as those used in Section 4.2. From Table 4, all the approximate circuits obtained by SEALS except mtp8 (resp. cla32) have smaller areas (resp. delays) than those by Su’s method. Compared with Su’s method, the runtime of SEALS is dramatically reduced. On average, SEALS is 15× faster than Su’s method.

Table 4: Comparison of SEALS and Su’s method under MRED constraint.

circuit	Average area ratio		Average delay ratio		Average time (s)	
	Su	SEALS	Su	SEALS	Su	SEALS
cla32	28.29%	25.93%	53.80%	61.33%	3583	276
ksa32	29.58%	28.66%	81.81%	75.70%	7839	356
mtp8	95.98%	97.03%	98.94%	95.70%	630	46
rca32	33.20%	31.87%	97.59%	92.39%	1418	164
wal8	94.95%	84.04%	93.60%	88.00%	1147	71
Avg	56.40%	53.72%	85.15%	86.55%	2924	191

5 CONCLUSION

In this work, we propose SEALS, a sensitivity-driven efficient ALS method to speed up a greedy ALS flow. Based on the newly proposed metric called sensitivity, we propose a fast and accurate error estimation method and an efficient LAC filtering technique to filter out some unpromising LACs. SEALS outperforms a state-of-the-art ALS method in runtime without reducing circuit quality.

REFERENCES

- [1] Q. Xu, T. Mytkowicz, and N. S. Kim. Approximate computing: A survey. *IEEE Des. Test*, 33(1):8–22, 2015.
- [2] S. Mittal. A survey of techniques for approximate computing. *ACM Comput. Surv.*, 48(4):62:1–62:33, 2016.
- [3] I. Scarabottolo, G. Ansaloni, et al. Approximate logic synthesis: A survey. *Proc. IEEE*, 108(12):2195–2213, 2020.
- [4] D. Shin and S. K. Gupta. A new circuit simplification method for error tolerant applications. In *DATE*, pages 1–6, 2011.
- [5] S. Venkataramani, K. Roy, and A. Raghunathan. Substitute-and-simplify: A unified design paradigm for approximate and quality configurable circuits. In *DATE*, pages 1367–1372, 2013.
- [6] J. Miao, A. Gerstlauer, and M. Orshansky. Multi-level approximate logic synthesis under general error constraints. In *ICCAD*, pages 504–510, 2014.
- [7] Z. Vasicek and L. Sekanina. Evolutionary approach to approximate digital circuits design. *IEEE Trans. on Evol. Comput.*, 19(3):432–444, 2015.
- [8] Y. Wu and W. Qian. An efficient method for multi-level approximate logic synthesis under error rate constraint. In *DAC*, pages 128:1–128:6, 2016.
- [9] A. Chandrasekharan, T. Villa, et al. Approximation-aware rewriting of AIGs for error tolerant applications. In *ICCAD*, pages 83:1–83:8, 2016.
- [10] G. Liu and Z. Zhang. Statistically certified approximate logic synthesis. In *ICCAD*, pages 344–351, 2017.
- [11] S. Hashemi, H. Tann, and S. Reda. BLASYS: Approximate logic synthesis using Boolean matrix factorization. In *DAC*, pages 55:1–55:6, 2018.
- [12] C. Meng, W. Qian, and A. Mishchenko. ALSRAC: Approximate logic synthesis by resubstitution with approximate care set. In *DAC*, pages 187:1–187:6, 2020.
- [13] J. Echavarría, S. Wildermann, and J. Teich. Approximate logic synthesis of very large Boolean networks. In *DATE*, pages 1552–1557, 2021.
- [14] S. Su, Y. Wu, and W. Qian. Efficient batch statistical error estimation for iterative multi-level approximate logic synthesis. In *DAC*, pages 54:1–54:6, 2018.
- [15] J. Echavarría, S. Wildermann, et al. Probabilistic error propagation through approximated Boolean networks. In *DAC*, pages 1–6, 2020.
- [16] I. Scarabottolo, G. Ansaloni, et al. Partition and propagate: an error derivation algorithm for the design of approximate circuits. In *DAC*, pages 1–6, 2019.
- [17] M. Hansen et al. Unveiling the ISCAS-85 benchmarks: a case study in reverse engineering. *IEEE Des. Test Comput.*, 16(3):72–80, 1999.
- [18] S. Yang. Logic synthesis and optimization benchmarks. Technical report, Microelectronics Center of North Carolina, 1991.